Research On Structure Design And Control Of Vehicle Platform Automatic Leveling System

Xing Zhuo Huang, Qi Yang*, Wei Jia Yan, Yang Tian, and Xun Yang Liang

Shenyang Ligong University, School of Mechanical

*Corresponding author. E-mail: yangqi@sylu.edu.cn

Received: December 05, 2023; Accepted: January 07, 2024

In the vehicle leveling system, due to the overall volume is too large and other reasons, the leveling speed is slow, the leveling range is small, and the adjustment stability is insufficient. According to the characteristics of the three-legged parallel robot, this paper designs a new structure which is superior to the traditional hydraulic straight up straight down leg structure, and is superior to the traditional leveling system in both the leveling range and accuracy. The three-point leveling method is selected, and the basic center point leveling algorithm is improved. After the basic leveling operation is completed, the fine adjustment is added to further reduce the position error and improve the leveling precision. At the same time, according to the new structure, the connection between the dynamic and static platform is analyzed, and the linkage module between the leveling platform, the connecting rod and the corresponding slider is established. Then, through the simulation of platform tilt, the data verification is carried out directly with the algorithm results to improve the inspection efficiency.This paper proposes and designs a small vehicle-mounted leveling system with novel structure to solve the problems of the leveling range and the lack of stability of the existing small leveling platform, and completes its structural design, algorithm optimization and algorithm feasibility verification. It is intended to provide a new reference direction for small vehicle leveling system.

Keywords: Leveling system; Leveling structure; Leveling algorithm; Algorithm detection

http://dx.doi.org/10.6180/jase.202411_27(11).0015

1. Introduction

In recent years, modern control theory, servo motor technology, and sensor technology have rapidly advanced, resulting in significant improvements in accuracy and speed of multi-point leveling systems. Emerging algorithms have gained popularity, and continuous innovation in structure and components has made multi-point leveling systems applicable to a wider range of applications, leading to continuous improvement in overall performance. These systems are commonly used in various scientific experiments and technological projects to provide a relatively stable experimental platform, such as urban rail network environment testing, assembly platforms for precision instruments including gears, experimental platforms for autonomous mobile robots and manipulators, high-quality experimental environments for optical linear encoders and computer vision. By utilizing leveling systems, these experiments can be conducted in a completely level environment, facilitating the acquisition of highly accurate experimental results [1–8].

Based on the current high standard and high requirements for the leveling system, the four major breakthrough goals should be to improve the leveling accuracy, improve the stability and quality of the leveling system, improve the leveling speed and improve the system operability, so as to improve the comprehensive ability of the automatic leveling system.Based on the characteristics of the three-legged

parallel robot, this paper designs the overall mechanical structure of the leveling system platform, which is better than the traditional hydraulic straight up straight down leg structure, and has better leveling range and accuracy than the traditional leveling system. The material selection, performance requirements, support mode and transmission mode of the whole structure are selected and studied in detail. The corresponding finite element analysis and dynamic analysis of the whole structure model are carried out. To ensure the operational viability of its structure. At the same time, the leveling principle of the structure is analyzed, and the overall structure design is completed [9].

The main leveling algorithms are analyzed deeply, and the advantages and disadvantages of the main leveling algorithms under the same conditions are analyzed. In addition, the conventional basic algorithm is strengthened and improved to eliminate position errors caused by factors such as motor delay as much as possible. The new leveling algorithm will have better performance in leveling accuracy. For the new structure, a linkage module is designed specially for this special structure, which is combined with the leveling algorithm to complete the leveling operation on the new structure according to the data of each sensor. A scheme to test the completed leveling algorithm is proposed. CAD software was used to establish a simple leveling platform for simulation to obtain the displacement data before and after each leveling point. After that, the completed algorithm is coded, and the corresponding software is used to simulate the angular rotation, and the data before and after the displacement are obtained. By comparing with the data obtained by manual rotation, the conclusion whether the algorithm is correct can be intuitively obtained [10].

Through a series of simulation experiments, the specific data and characteristic display of the leveling system designed in this paper are confirmed. It includes the limit test of the leveling Angle, the degree of improvement of the improved algorithm to reduce the position error under the condition of 20°, the simulation comparison experiment of the feasibility analysis of the algorithm, and the data comparison with the leveling scheme proposed by foreign scholars. The purpose of this paper is to solve the problems such as many structural defects, slow leveling speed and small working range, and to provide more references and directions for the research of small leveling stations [11–14].

2. Theory and formula

2.1. Composition of multi-point leveling system

Multi-point leveling system is currently widely used in the world in the military, infrastructure, medical, rescue, exploration and other fields of the work platform support and leveling system, most of the current automatic leveling system is composed of the main controller, driver, tilt sensor, and the corresponding number of legs, of which, when the number of legs is three, this institution is called three-point leveling. In addition to the three-point leveling, the four-point leveling and six-point leveling of the four legs are the most common, and the drive system is divided into electromechanical leveling and hydraulic leveling [15].

The working principle of the multi-point leveling system is actually that the main controller receives the tilt Angle information of the X axis and Y axis direction output by the tilt Angle sensor or gyroscope. After the calculation of the leveling algorithm, the extension and extension of each leg are controlled by the corresponding driving system. Finally, the X-axis inclination Angle and Y-axis inclination Angle on the working platform can reach the horizontal accuracy required by the work, so as to complete the corresponding platform leveling operation [16].

2.2. Overall structure design

In this chapter, the overall mechanical structure of the leveling system platform is designed, and the corresponding finite element analysis and dynamic analysis are carried out to ensure the feasibility of its structural operation. It includes a detailed analysis of its material selection, performance requirements, support mode, transmission mode.

The overall three-dimensional structure consists of a base and three leveling bases as the main body, and the transmission mechanism inside the base connects the slider, and then connects two connecting rods through the ball-type link, and the other end is connected to the leveling table. The inclination sensor is installed on the base, and the transmission mechanism is driven by the motor to drive the sliding movement, so as to complete the leveling operation of the platform. Double support beams are added to the base part to ensure its stiffness and balance, and the spherical link ensures that the platform can be operated at a large enough Angle in the leveling operation. The two-link design enhances the system stiffness and avoids the interference problem caused by the single rod spherical link, which is superior to the traditional hydraulic leveling system in both the leveling range and accuracy. The comparison of the state of the overall three-dimensional structure before and after balance is shown in Fig. 1.

2.3. Choice of transmission mode

As the actuator of the whole system, the transmission mechanism has a great impact on the leveling accuracy and speed of the system. The selection of the appropriate trans-

Fig. 1. Comparison of the state before and after equilibrium of the 3D structure.

mission mechanism can accurately execute the movement according to the instruction issued by the controller, and realize the rapid and smooth leveling.According to the advantages and disadvantages of the common transmission scheme, the screw transmission in the screw transmission is selected as the leveling mechanism [17].

The design of this leveling system needs to be equipped with self-locking function, and the lead screw mechanism has good self-locking property in the horizontal state. In the structural model design, the three-position leveling mechanism designed in this paper is also better integrated, and the overall meets the requirements of the small leveling system for accuracy, strength and self-locking function. The simple lead screw mechanism to be designed is shown in Fig. 2.

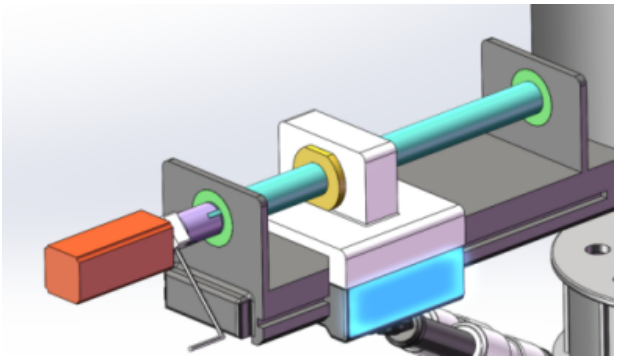

Fig. 2. Simple lead screw mechanism.

2.4. Working principle of leveling

Based on the conventional three-legged parallel robot structure, a new structure is designed which is superior to the traditional hydraulic straight up and straight down legs. It is composed of leveling base, sliding block guide rail, moving platform, double support connecting rod and corresponding driving system. The structural schematic diagram is shown in Fig. 3. In the figure, B12, B34, B56 are the sliding blocks on the leveling base, A1, A2, A3, A4, A5, A6 are the leveling platform, and A1B1-A6B6 are the equilateral triangle formed by three links between the moving platform and the slider A12, A34, A56 as a simple moving

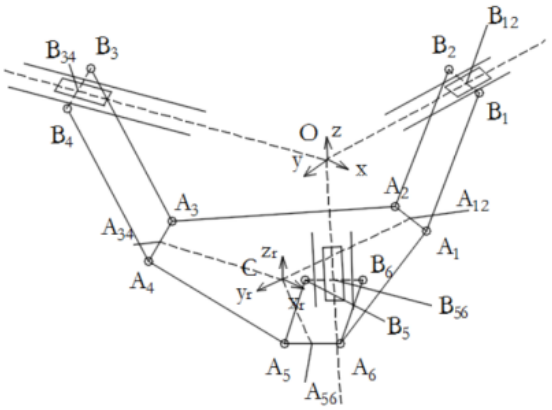

Fig. 3. Schematic diagram of three-point support platform structure.

platform for analysis. The end point of the moving platform, the connecting rod, and the slider are all connected by ball links to ensure that they can work at multiple angles.

The working principle is: The sensor receives the inclination data of the current environment and transmits it to the control system. The control system calculates the corresponding amount of exercise of the six connecting rods through the leveling algorithm, and then calculates the corresponding amount of exercise of the slide block through the corresponding linkage module of the moving platform and the guide rail. After that, the data is transferred to the servo motor, which drives the slide block to move to the corresponding position. Drive the connecting rod to balance the platform, so as to complete the leveling operation.The flowchart of its working principle is shown in Fig. 4.

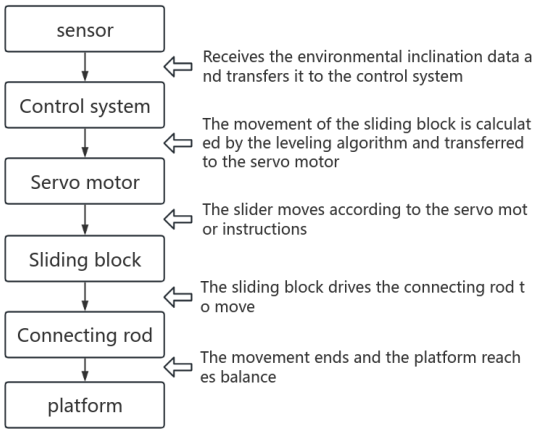

Fig. 4. Work flow chart of leveling system.

Table 1. Specific parameters of high-carbon alloy steel.

Stats	Numerical value	unit
Elastic inertia	2.10E + 11	N/m^2
Poisson's ratio	0.28	
Shear modulus	7.90E + 10	N/m^2
Mass density	7700	kg/m^3
Tensile strength	723825600	N/m^2
Yield strength	620433000	N/m^2
Coefficient of thermal expansion	1.3w − 05	K
Thermal conductivity	50	W/(m.K)
Specific heat	460	J/(kg.K)

2.5. Structural material selection

According to the analysis and selection of the current mainstream metal materials, the leveling mechanism and its corresponding connection parts are made of high carbon alloy steel.

In high-carbon alloy steel, the internal carbon content increases, the tensile strength and yield point will increase, with high hardness and high wear resistance, etc., suitable for the levelling chassis of the connection vehicle, the base of the support platform, and the main stress bearing connecting rod. At the same time, with the increase of carbon content, when the carbon content of high-carbon alloy steel exceeds 0.23%, its welding performance will be decreased, but the leveling mechanism designed in this paper adopts the form of multi-part assembly, which requires fewer parts to be welded, and will not be affected by this shortcoming.The specific parameters of the high-carbon alloy steel used are shown in Table 1.

2.6. Finite Element Analysis

This time, Ansys workbench version 19.0 was used to perform the base strength check analysis, including statics analysis and modal analysis. The inclined rod is subjected to 300N load. The final analysis results obtained are shown in Fig. 5 and Fig. 6.

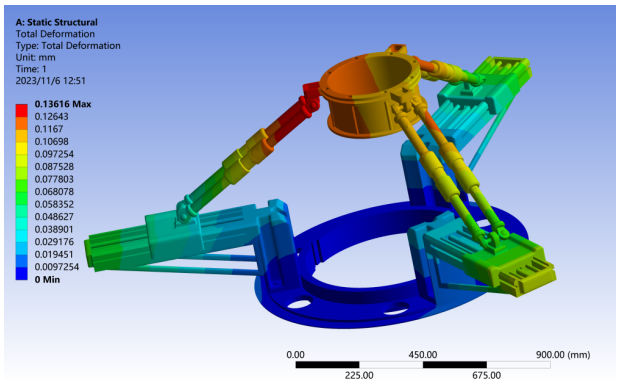

Fig. 5. Summary of total deformation cloud map.

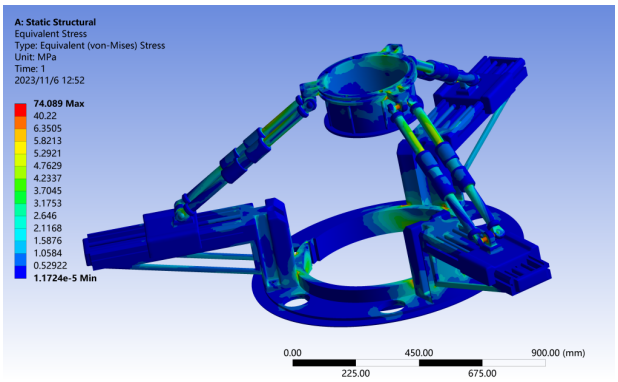

Fig. 6. Equivalent stress cloud map.

It can be seen from the deformation cloud map that the maximum deformation is 0.13616 mm, which is almost negligible for the whole system. The stress nephogram shows that the maximum stress is 74.089 MPa. The maximum stress of alloy steel is 250 MPa, which is far from reaching the yield strength of alloy steel, so it is considered safe. The security factor cloud map shows that most of them are blue areas, and all of them are above 1, proving that they are all safe.

2.7. Dynamic Analysis

Before the material is given, the steps are the same as the finite element analysis, the mesh is divided, the constraints are applied, and then the contact between the slider and the track is modified to frictional contact. Next, the load is applied and, in this analysis, the slider is set to move inward along the track by a distance of 30mm. The final analysis results obtained are shown in Fig. 7 and Fig. 8.

It can be seen from the deformation cloud image that the maximum displacement is 30.439mm. For the base, the displacement is moved from the original position of the slider to the target position, and the displacement is only 0.439 mm. The influence of the displacement on the whole mechanism is almost negligible.

The stress cloud map shows that the maximum stress is

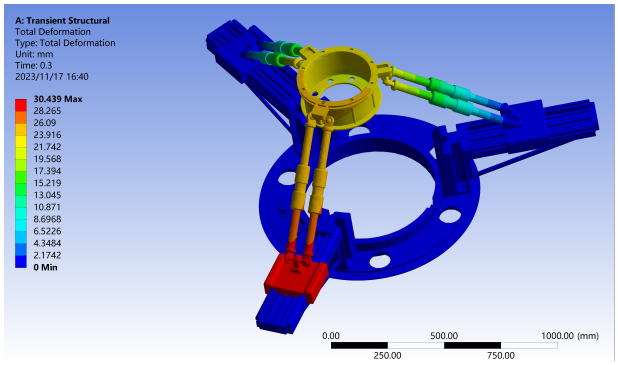

Fig. 7. Total deformation cloud diagram.

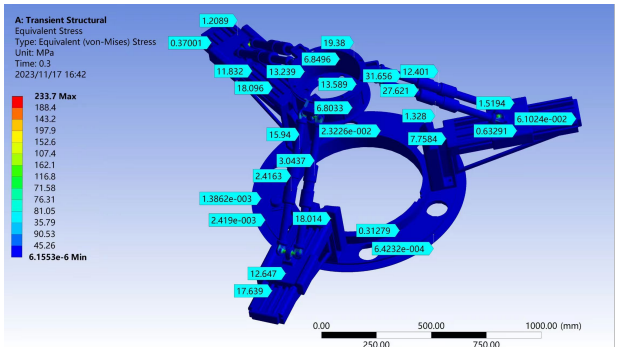

Fig. 8. Equivalent stress cloud map.

233.7 MPa and the minimum stress is almost 0. The results show that the stress in the whole area is less than the yield strength of 250 MPa, and the maximum stress of alloy steel is 250 MPa, which is within the strength range for the yield strength of alloy steel, so it is considered safe.

2.8. Platform kinematics analysis

Through the research, it is found that the body of the leveling system is its corresponding working platform, and the analysis of the platform can be regarded as a simple plane, and the analysis of the plane leveling data can replace the whole platform. As shown in Fig 9. Taking the three-point platform as an example, the Angle between the plane ABC and X0 is α, and the Angle between the plane and Y0 is β. Meanwhile, X0Y0Z0 is the horizontal coordinate system, and the corresponding platform coordinate system XYZ is established on this plane. We can assume that the operating platform timing only rotates under an ideal state. The leveling of the platform can be seen as the process of the plane ABC first rotating the α Angle about the Y axis and then rotating the β Angle about the X axis. Therefore, the coordinate of each support point in the horizontal coordinate system after two rotations can be obtained by establishing the pose transformation matrix [18]. Let A point on the

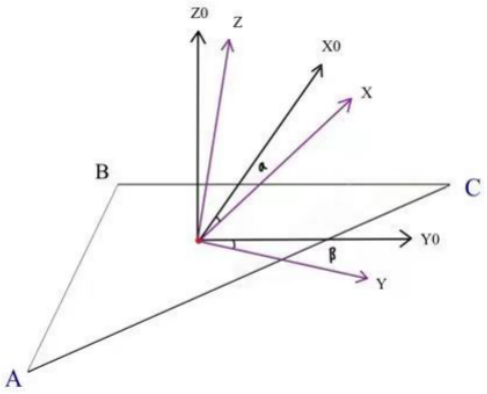

Fig. 9. Simple three-point platform leveling analysis.

platform be (x, y, z), when the Angle of α is rotated around the Y axis, the coordinate becomes (x_1, y_1, z_1), then:

$$(x_1, y_1, z_1) = \mathrm{ROT}(Y, \alpha)(x, y, z)^T = \begin{bmatrix} \cos\alpha & 0 & \sin\alpha \\ 0 & 1 & 0 \\ -\sin\alpha & 0 & \cos\alpha \end{bmatrix} (x, y, z)^T \quad (1)$$

Continue to rotate the Angle about the X-axis, the coordinate becomes (x_2, y_2, z_2), then there is:

$$(x_2, y_2, z_2) = \mathrm{ROT}(X, \beta)\,(x_1, y_1, z_1)^T = \begin{bmatrix} 1 & 0 & 0 \\ 0 & \cos\beta & \sin\beta \\ 0 & -\sin\beta & \cos\beta \end{bmatrix} (x_1, y_1, z_1)^T \quad (2)$$

By bringing equation Eq. (1) into equation Eq. (2), the pose transformation matrix representing the two conversion processes of platform rotation can be obtained:

$$(x_2, y_2, z_2)^T = \mathrm{ROT}(X, \beta)\,\mathrm{ROT}(Y, \alpha)(x, y, z)^T = \begin{bmatrix} \cos\alpha & 0 & \sin\alpha \\ -\sin\alpha\sin\beta & \cos\alpha & \cos\alpha\sin\beta \\ -\sin\alpha\cos\beta & -\sin\beta & \cos\alpha\cos\beta \end{bmatrix} (x, y, z)^T \quad (3)$$

Therefore, the coordinate of each support point $(x_i', y_i', z_i')^T$ in the horizontal coordinate system is $\mathrm{ROT}\,(x_i, y_i, z_i)^T$, To facilitate calculation, let the displacement of each point in the space coordinate z-axis be 0 , then:

$$\begin{bmatrix} x_i' \\ y_i' \\ z_i' \end{bmatrix} = \begin{bmatrix} \cos\alpha & 0 & \sin\alpha \\ -\sin\alpha\sin\beta & \cos\alpha & \cos\alpha\sin\beta \\ -\sin\alpha\cos\beta & -\sin\beta & \cos\alpha\cos\beta \end{bmatrix} \begin{bmatrix} x_i \\ y_i \\ 0 \end{bmatrix} \quad (4)$$

Table 2. Specific parameters of high-carbon alloy steel.

Leveling method	Leveling time	Leveling time
Leveling method by height	6.5 S	230 mm
Lower and lower leveling method	6.5 S	230 mm
Center point stationary leveling method	4.5 S	260 mm
Set point stationary leveling method	6.5 S	130 mm

Therefore, we can obtain:

$$z_i' = -\sin\alpha\cos\beta x_i' - \sin\alpha y_i' \tag{5}$$

In addition, because the inclination of multi-point platforms is usually relatively small, it can be approximated as $\sin\alpha = \alpha, \cos\alpha = \alpha, \sin\beta = 1, \cos\beta = 1$.Formula 3 can be simplified as:

$$(x_2, y_2, z_2)^T = \begin{bmatrix} 1 & 0 & \alpha \\ 0 & 1 & \beta \\ -\alpha & -\beta & 1 \end{bmatrix} (x, y, z)^T \tag{6}$$

After simplification, we get:

$$z_i' = -\alpha x_i - \beta y_i \tag{7}$$

The above formula represents the relationship between the position error of each support point reaching the horizontal state and its corresponding inclination Angle after simplification.

2.9. Basic leveling algorithm selection

There are four main leveling methods, which are the leveling method by height, the leveling method by low, the leveling method without moving the center point, and the leveling method without moving the set point. For the convenience of comparison, the value of α_0, β_0 is set to 1, M=80 mm, N=100 mm, and V=20 mm/s, and the comparison data of each leveling method is obtained by reducing the leveling time and adjusting the distance under the same conditions, as shown in Table 2.The method used in this comparison experiment is to build a general leveling table, and set the tilt Angle and motor speed values to the same values, and test the results under the same conditions and workload [19, 20].

By comparing the data, among several leveling methods, the leveling time and adjusting distance of the height-by-height leveling method and the low-by-height leveling method are completely consistent, but there are differences in the square adjustment direction. The absolute value of the data is relatively large, and the two data of the central point immobile leveling method are the best. Therefore, in the selection of leveling algorithm, the central point immobile leveling method can be preferentially selected.

2.10. Establishment of linkage module between moving platform and guide rail

After obtaining the coordinate of the leveling change of the connecting hinge points A_{12}, A_{34} and A_{56} of the moving platform and the leveling mechanism through the transformation matrix, it is also necessary to analyze the corresponding feed amount of the three sliders connected by the connecting rod of the static platform during the leveling process of the moving platform according to the structural particularity of the system. Since the distance between A_{12}, A_{34}, A_{56} and B_{12}, B_{34} and B_{56} is a rod length of 633 mm, we can first find the correspondence between the moving platform coordinate system and the static platform coordinate system, and then reverse the coordinates of B_{12}, B_{34} and B_{56} through the distance formula of two points in space, and finally obtain the length change values of B_{12}, B_{34} and B_{56}.

If the distance from the origin of the platform coordinate system to the end of the base is set to K, it is known that the initial coordinates of the three points of the equilateral triangle ABC representing the leveling platform are shown in Equation Eq. (8).

$$\begin{aligned} A_{12} &= (0, -K, 0) \\ A_{34} &= \left(-\frac{K\sqrt{3}}{2}, \frac{K}{2}, 0\right) \\ A_{56} &= \left(\frac{K\sqrt{3}}{2}, \frac{K}{2}, 0\right) \end{aligned} \tag{8}$$

The corresponding coordinates after two rotations are shown in equation Eq. (9).

$$\begin{aligned} A_{12} &= (0, K\cos\alpha, K\sin\alpha) \\ A_{34} &= \left(\frac{K\sqrt{3}}{2}\cos\beta, \frac{K\sqrt{3}}{2}\sin\alpha\sin\beta - \frac{K}{2}\cos\alpha,\right. \\ &\left. -\frac{K\sqrt{3}}{2}\sin\beta\cos\alpha - \frac{K}{2}\sin\alpha\right) \\ A_{56} &= \left(-\frac{K\sqrt{3}}{2}\cos\beta, -\frac{K\sqrt{3}}{2}\sin\alpha\sin\beta - \frac{K}{2}\cos\alpha,\right. \\ &\left. \frac{K\sqrt{3}}{2}\sin\beta\cos\alpha - \frac{K}{2}\sin\alpha\right) \end{aligned} \tag{9}$$

By re-establishing coordinate system O on the static platform where the three sliders are located, the conversion

relationship between the two coordinate systems can be obtained as follows:

$$(x, y, z) = (-z\sin\beta, +z\sin a, z\sqrt{1-\sin\alpha\sin\alpha-\sin\beta\sin\beta}) \tag{10}$$

Therefore, the coordinates of three points A_{12} A_{34} A_{56} with respect to the O-coordinate system are shown in equation 11 .

$$\begin{aligned}
A_{12} =& (K\sin\alpha\sin\beta - z\sin\beta, K\cos\alpha + z\sin\alpha, K\sin\alpha \\
& - z\sqrt{1-\sin\alpha\sin\alpha-\sin\beta\sin\beta}) \\
A_{34} =& \left(\frac{K\sqrt{3}}{2}\cos\beta - z\sin\beta,\right. \\
& \left(\frac{K\sqrt{3}}{2}\sin\alpha\sin\beta - \frac{K}{2}\cos\alpha\right) + z\sin\alpha, \\
& \left(-\frac{K\sqrt{3}}{2}\sin\beta\cos\alpha - \frac{K}{2}\sin\alpha\right) \\
& \left.-z\sqrt{1-\sin\alpha\sin\alpha-\sin\beta\sin\beta}\right) \\
A_{56} =& \left(-\frac{K\sqrt{3}}{2}\cos\beta - z\sin\beta,\right. \\
& \left(-\frac{K\sqrt{3}}{2}\sin\alpha\sin\beta - \frac{K}{2}\cos\alpha\right) + z\sin\alpha, \\
& \left(\frac{K\sqrt{3}}{2}\sin\beta\cos\alpha - \frac{K}{2}\sin\alpha\right) \\
& \left.-z\sqrt{1-\sin\alpha\sin\alpha-\sin\beta\sin\beta}\right)
\end{aligned} \tag{11}$$

The coordinates of sliders B_{12}, B_{34}, and B_{56} with respect to the O-coordinate system are shown in equation Eq. (12).

$$\begin{aligned}
B_{12} &= (0, y_{12}, 0) \\
B_{34} &= (x_{34}, -x_{34}, 0) \\
B_{56} &= (x_{56}, x_{56}, 0)
\end{aligned} \tag{12}$$

The slider position at the beginning is shown in equation Eq. (13).

$$\begin{aligned}
B_{12} &= (0, -1.94K, 0) \\
B_{34} &= (-1.53K, 0.97K, 0) \\
B_{56} &= (1.53K, 0.97K, 0)
\end{aligned} \tag{13}$$

Because the distance between A_{12}, A_{34}, A_{56} and B_{12}, B_{34}, B_{56} is always L; According to the formula of distance between two points in space:

$$\sqrt{(x_1-x_2)^2+(y_1-y_2)^2+(z_1-z_2)^2} = L \tag{14}$$

The coordinates of the inverse solution B_{12}, B_{34} and B_{56} in the O-coordinate system are shown in equation Eq. (15).

$$\begin{aligned}
B'_{12} &= (0, y'_{12}, 0) \\
B'_{34} &= \left(x'_{34}, -\frac{\sqrt{3}}{3}x'_{34}, 0\right) \\
B'_{56} &= \left(x'_{56}, \frac{\sqrt{3}}{3}x'_{56}, 0\right)
\end{aligned} \tag{15}$$

Then Value range of y' is $(1.48\,\mathrm{K}, 2.4\,\mathrm{K})$, $\frac{\sqrt{3}}{3}x'$ value range $(0.74\,\mathrm{K}, 1.2\,\mathrm{K})$, deflection Angle range 19.93° Due to the motion delay of the motor used in the mechanical system and the influence of a small amount of friction, the final position of the slider may be slightly different from the final value of the algorithm. This deviation factor will be expressed as δ and will be eliminated in the fine-tuning steps mentioned below.

Since the slider B_{12} sliding center slides on the negative half axis of the Y-axis. Sliding distance is: $\Delta B_{12} = y' + 1.94K + \delta$.

$\Delta B_{12} \geq 0$, The slider moves toward the positive half of the Y-axis. $\Delta B_{12} < 0$, The slider moves toward the negative half of the Y-axis.

The distance between the slider B_{34} and the O point after sliding is: $-\frac{2\sqrt{3}}{3}x'_{34}$ The sliding distance of slider B_{34} is : $\Delta B_{34} = \frac{2\sqrt{3}}{3}x + 1.94K + \delta$.

$\Delta B_{34} \geq 0$, The slider moves in the direction O away from the center. $\Delta B_{34} < 0$, The slider moves in the direction O near the center.

The distance between the slider B56 and point O after sliding is: $\frac{2\sqrt{3}}{3}x'_{56}$ The sliding distance of slider B_{56} is : $\Delta B_{56} = -\frac{2\sqrt{3}}{3}x + 1.94K + \delta$.

$\Delta B_{56} \geq 0$, The slider moves in the direction O away from the center. $\Delta B_{56} < 0$, he slider moves in the direction O near the center.

2.11. Loop fine-tuning algorithm

Due to the inherent delay of the motor and a small amount of friction in the mechanical structure, there are still some differences between the actual and expected leveling results based on the algorithm. In order to increase the leveling accuracy, this paper improved the conventional center point leveling algorithm in a deeper way. After the completion of the conventional leveling operation, there would still be a large position error at each support point, so the conventional leveling operation was defined as rough adjustment. In order to eliminate the position error as much as possible, fine adjustment steps could be added to the original algorithm [21].

It consists of the position error e_i, the leveling speed v_i, the speed coefficient k, and the single fine-tuning time t.

After entering the fine adjustment, the speed coefficient is set between 0.1-1 according to the accuracy requirements, and the new error after fine adjustment is obtained by calculating $e_{i+1} = e_i - kv_i t$. Set E1 as the position error threshold, if $e_{i+1} > E1$, repeat the fine adjustment step until the fine adjustment is finished at $e_{i+1} < E1$, and the position error is greatly reduced compared with before. The leveling flow chart after the algorithm improvement is shown in Fig. 10.

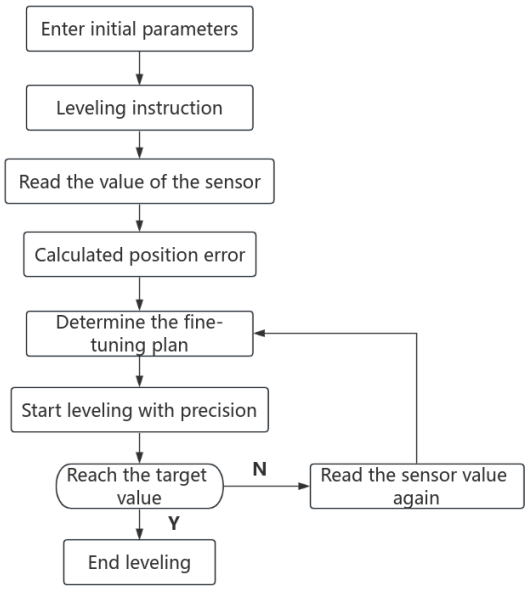

Fig. 10. Overall leveling flowchart.

3. Experimental and result

3.1. Confirmation of maximum leveling Angle

According to the final design of the leveling system model, the leveling Angle range of the platform is tested. According to the working principle of the leveling platform, a simple cylindrical static platform is added into the whole three-dimensional structure, and the maximum bending Angle of the leveling platform is determined by the interference detection between the platform and the chassis edge. The limit inclination Angle without interference is taken as the maximum value, and the corresponding two-dimensional drawing is derived to determine the range of leveling Angle. The final leveling range is 0-19.93°. Most of the leveling angles of traditional straight up and straight down leveling structures are 5°-10°. A two-dimensional drawing showing the maximum Angle is shown in Fig. 11.

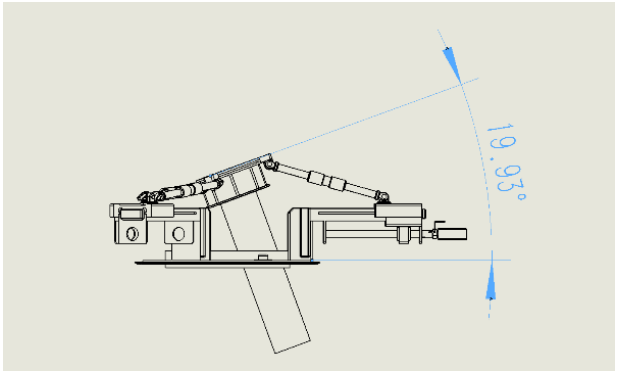

Fig. 11. Maximum range of leveling Angle.

3.2. Algorithm feasibility analysis simulation experiment

This paper proposes to design a method to verify the completed algorithm by combining two software, draw a simple platform model through simulation, manually simulate the rotation of the corresponding Angle, and obtain the position data of each point after the displacement is completed. At the same time, the completed algorithm was programmed and run through pycharm software to obtain the specific position data after leveling. If the two data are the same, it is correct, which significantly improves the feasibility verification of the leveling system algorithm. The simple platform simulation is shown in Fig. 12.

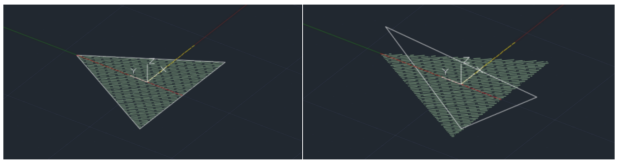

Fig. 12. The initial state of the platform is transformed into 20 states of rotation of each XY axis.

Input the central point leveling algorithm obtained above, and test the space position of each support point of the platform after rotating $\alpha = 20°$ on the X-axis and $\beta = 20°$ on the Y-axis. See Table 3, Table 4 and Table 5.

Table 3. Position data of support point A when the two axes are rotated 20.

Point A	Simulation data	Algorithm data
X	0	0
Y	186.1955	186.1954
Z	107.5000	107.4999

By comparing the data, the position data of the three points of the three-point platform is completely consistent with the data obtained in the algorithm simulation and

Table 4. Position data of support point B when the two axes are rotated 20.

Point B	Simulation data	Algorithm data
X	161.2500	161.2500
Y	-46.5489	-46.5488
Z	-134.3750	-134.3750

Table 5. Position data of support point C when the two axes are rotated 20.

Point C	Simulation data	Algorithm data
X	-161.2500	-161.2500
Y	-139.6466	-139.6466
Z	26.8750	26.8750

simulation simulation. In order to prove its reliability, a set of data is tested again, which are different rotation angles of $\alpha = 35°$ and $\beta = 17°$ respectively. The experimental data pairs are shown in Table 6,7 and 8. The data are consistent and fully meet the accuracy requirements.

Table 6. Position data of support point A when the two axes rotate 5.

Point A	Simulation data	Algorithm data
X	0	0
Y	214.18	214.2
Z	18.74	18.7

Table 7. Position data of support point B when the two axes rotate 5.

Point B	Simulation data	Algorithm data
X	185.49	185.5
Y	-105.67	-105.7
Z	-25.53	-25.5

Table 8. Position data of support point C when the two axes rotate 5.

Point C	Simulation data	Algorithm data
X	-185.48	-185.5
Y	-108.5	-108.5
Z	6.79	6.8

3.3. Fine-tuning simulation experiment

The position error after leveling is output by using a simple CAD platform and a cyclic fine-tuning algorithm. According to the accuracy requirements, the speed coefficient is set between $0.1 - 1$, and the new error after fine adjustment is obtained by calculating $e_{i+1} = e_i - kv_i t$. When the platform inclination $\alpha = 20°, \beta = 20°$, after four fine-tuning processes, the ABC three-point position error is shown in Fig 13. It is obvious that while the velocity coefficient is decreasing, the position error shows a reverse exponential trend and finally tends to be relatively stable. Where the abscissa represents the number of times the precise leveling is performed, and the ordinate represents the current position error.

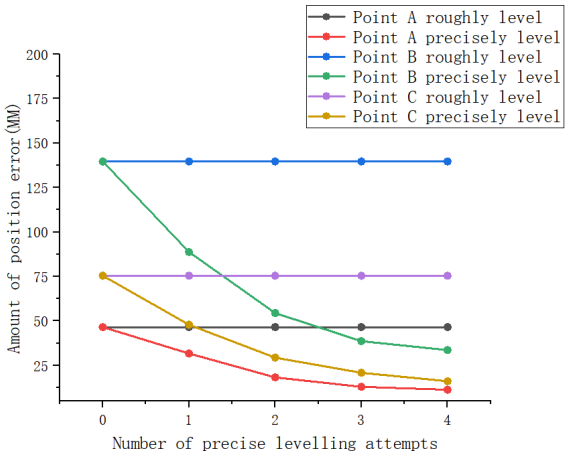

Fig. 13. Three point position error variation.

3.4. Comparison with similar leveling systems

Literature [22] proposes a two-degree-of-freedom wheeled vehicle leveling mechanism suitable for small working vehicles. The system can be used in various transportation equipment, conveying and stabilizing systems. The platform can rotate freely with the help of the ball-and-socket joint in its center. The lateral and longitudinal movements are controlled by two servo motors. When the vehicle is driving on slopes or rough terrain, the instantaneous tilt of the platform is measured by a gyroscope, making it particularly suitable for outdoor work.

Literature [23] proposes a two-wheel self-stabilizing leveling mechanism, which uses two DC motors to match the driver and Arduino UNO microcontroller board. The value of the tilt Angle is obtained by the IMU and fed to the PID controller to control the balance of the drive motor in the system.

The levelling mechanism designed in this paper is used to carry out the next experiment, and the platform is levelled at an inclination of 1° to test the levelling time under this workload. According to the data obtained by the sensor, the leveling algorithm and linkage algorithm in this paper, together with the parameters of the servo motor, can obtain the time required for the platform balance when the Angle of the platform is 1°. According to the position error after four times of fine adjustment obtained by the

Table 9. Comparison of experimental data between the leveling mechanism designed in this paper and other leveling mechanisms.

method	Reference [22] methods	Reference [23] Methods	Textual method
Maximum tilt Angle	5°	5°	19.93°
Leveling time when the single leveling Angle is 1	140 ms	235 ms	100.3 ms
Leveling Angle error	$< 1°$	$< 2°$	$< 0.3°$

simulation experiment of fine adjustment, the Angle error after finishing the leveling operation can be obtained by comparing with the data of the inclination sensor.

According to the experimental data in literature [22] and [23], the specific comparison with the small three-point leveling mechanism proposed in this paper in terms of levelling time, levelling range, and whether there are additional problems in the same proportion of levelling workload is shown in Table 9.

By comparing the data with the two foreign mainstream leveling equipment, the leveling speed and accuracy are slightly higher than those in the literature [22] and [23], and the leveling range is greatly improved compared with the other two methods.

4. Discussion

Although this paper presents a small three-point leveling system that meets the design requirements, some problems remain unsolved. Since the mathematical modeling of the platform in this paper is based on the premise that the levelling table, the supporting link and the working environment are all rigid, that is to say, the levelling table, the supporting link and the working environment will not produce deformation enough to affect the result when the force is acted on. However, when the actual leveling platform, supporting connecting rod and working environment are subjected to force, corresponding deformation will occur, and the deformation has a certain impact on the performance of the leveling system, and even the platform can not be adjusted to balance in serious cases. Although the corresponding statics analysis of the leveling mechanism has been done in this paper and its usability has been confirmed, there are no specific requirements for its working environment. Therefore, it is necessary to further analyze the working environment of the platform and establish a more accurate application system.

5. Conclusions

Designed a different from traditional leveling system based on a tripod, a novel parallel robot, so that it can be widely applicable to environment, can meet the demand of more leveling. The structure is more lightweight, the leveling speed is faster, and the application range is wider. Compared with the old structure, the structure designed in this paper provides superior horizontal range and institutional flexibility. In terms of comprehensive performance, the proposed structure is superior to the traditional leveling system.

Put forward a more advanced level algorithm, through to the finer leveling operation to carry on the multiple iterations, rapidly improve the leveling accuracy. In addition, the linkage module is also designed for the leveling structure, which is the result of the analysis and design of the structure in this paper, and is not suitable for the conventional leveling device of the standard structure.

Design a more efficient algorithm validation protocols. Through modeling the platform tilt, two sets of simulation data are obtained through physical simulation and digital derivation of platform model. The results of the two sets of data are directly compared for data-driven validation. This method avoids the low precision and low efficiency of manual repeated calculation, significantly improves the accuracy of algorithm verification, and effectively reduces the time required for verification.

The purpose of this study is to provide a new reference for the design of automatic leveling control system for vehicles and other small devices. The aim is to solve the various limitations caused by the traditional single leveling structure. This study improves the level of leveling system from the aspects of structure, algorithm and verification. It has certain significance for the development of small levelling device in civil field.

Funding

Liaoning Province's first major science and technology project, 2021020430-JH1/104

Acknowledgments

Thanks to my editorial staff Xue.Zhao for their guidance and help with the article layout.

References

[1] M. Taranetz, T. Blazek, T. Kropfreiter, M. K. Müller, S. Schwarz, and M. Rupp, (2015) *"Runtime precoding: Enabling multipoint transmission in LTE-advanced system-level simulations"* **IEEE Access** ***3***: 725–736. DOI: 10.1109/ACCESS.2015.2437903.

[2] R. Tsvetkov, V. Yepin, and A. Shestakov. "Numerical estimation of various influence factors on a multipoint hydrostatic leveling system". In: *IOP Conference Series: Materials Science and Engineering*. ***208***. 1. IOP Publishing. 2017, 012046. DOI: 10.1088/1757-899X/208/1/012046.

[3] J. Wang, J. Zhao, W. Cai, W. Li, X. Jia, and P. Wei, (2021) *"Leveling control of vehicle load-bearing platform based on multisensor fusion"* **Journal of Sensors** ***2021***: 1–7.

[4] L. Guo, H. Tan, and M. Zeng. "Design of Automatic Leveling Control System for Special Vehicle-mounted Platform". In: *2022 International Conference on Artificial Intelligence and Computer Information Technology (AICIT)*. IEEE. 2022, 1–5. DOI: 10.1109/AICIT55386.2022.9930164.

[5] S. Lee, J. Kawk, and B. Chu, (2020) *"Study of a leveling mobile platform for take-off and landing of unmanned aerial vehicles"* **Journal of the Korean Society of Manufacturing Process Engineers** ***19***(4): 85–92. DOI: 10.14775/ksmpe.2020.19.04.085.

[6] W. Jianjun, Z. Jingyi, L. Wenlei, C. Wei, and W. Yongchang. "The Study and Engineering Application on Adaptive Leveling of Vehicle Platform". In: *2019 International Conference on Advances in Construction Machinery and Vehicle Engineering (ICACMVE)*. IEEE. 2019, 285–290. DOI: 10.1109/ICACMVE.2019.00062.

[7] W. Tan, P. Liu, X. Li, S. Xu, Y. Chen, and J. Yang, (2022) *"Segmentation of lung airways based on deep learning methods"* **IET Image Processing** ***16***(5): 1444–1456. DOI: 10.1049/ipr2.12423.

[8] Z. Zhang, W. Tan, Y. Sun, J. Han, Z. Wang, H. Xue, and R. Wang, (2023) *"Self-supervised neural network-based endoscopic monocular 3D reconstruction method"* **Health Information Science and Systems** ***12***(1): 4. DOI: 10.1007/s13755-023-00262-7.

[9] D. Li, G. Ma, and J. Li, (2021) *"Four-point dynamic leveling method for drilling platform application"* **Assembly Automation** ***41***(2): 144–154. DOI: 10.1108/AA-02-2020-0021.

[10] L. Tan, B. Wu, V. Sood, D. Xu, M. Narimani, Z. Cheng, and N. R. Zargari, (2017) *"A simplified space vector modulation for four-level nested neutral-point clamped inverters with complete control of flying-capacitor voltages"* **IEEE Transactions on Power Electronics** ***33***(3): 1997–2006. DOI: 10.1109/TPEL.2017.2697847.

[11] R. B. Jiao, C. Chen, M. Yuan, and F. P. Wang, (2014) *"The study of automatically leveling control system on electromechanical vehicle stable platform"* **Applied Mechanics and Materials** ***494***: 266–269. DOI: 10.4028/www.scientific.net/AMM.494-495.266.

[12] A. Liu, J. Wu, F. Zhang, W. Yang, H. Wang, and X. Gang, (2023) *"Studies on a statically determinate leveling control strategy for a statically indeterminate four-leg support vehicle-borne platform"* **Mechanics Based Design of Structures and Machines** ***51***(12): 7131–7148. DOI: 10.1080/15397734.2022.2091593.

[13] K. Iturralde, M. Feucht, D. Illner, R. Hu, W. Pan, T. Linner, T. Bock, I. Eskudero, M. Rodriguez, J. Gorrotxategi, et al., (2022) *"Cable-driven parallel robot for curtain wall module installation"* **Automation in Construction** ***138***: 104235. DOI: 10.1016/j.autcon.2022.104235.

[14] Z. Chong, F. Xie, X.-J. Liu, J. Wang, and H. Niu, (2020) *"Design of the parallel mechanism for a hybrid mobile robot in wind turbine blades polishing"* **Robotics and Computer-Integrated Manufacturing** ***61***: 101857. DOI: 10.1016/j.rcim.2019.101857.

[15] V. L. Nguyen, C.-Y. Lin, and C.-H. Kuo, (2020) *"Gravity compensation design of Delta parallel robots using gear-spring modules"* **Mechanism and Machine Theory** ***154***: 104046. DOI: 10.1016/j.mechmachtheory.2020.104046.

[16] W.-a. Cao, D. Yang, and H. Ding, (2018) *"A method for stiffness analysis of overconstrained parallel robotic mechanisms with Scara motion"* **Robotics and Computer-Integrated Manufacturing** ***49***: 426–435. DOI: 10.1016/j.rcim.2017.08.014.

[17] E. L. M.E. Lustenkov B.B. Skaryno, (2019) *"Selection of an Asynchronous Motor for the Belt Conveyor Drive with a Parallel-Shaft Gearbox"* **Proceedings of Higher Educational Institutions Machine Building** (2 (707)): 3–10.

[18] S. Sawada, K. Kobayashi, H. Okada, and M. Katayama. "Selective transmission of control information based on channel periodicity in PLC-based multiple-machine control". In: *2017 IEEE International Symposium on Power Line Communications and*

its Applications (ISPLC). IEEE. 2017, 1–6. DOI: 10.1109/ISPLC.2017.7897109.

[19] G. Madhumitha, R. Srividhya, J. Johnson, and D. Annamalai. "Physical modeling and control of self-balancing platform on a cart". In: *2016 International Conference on Robotics: Current Trends and Future Challenges (RCTFC)*. IEEE. 2016, 1–6. DOI: 10.1109/RCTFC.2016.7893410.

[20] M. X. Gao and J. P. Bai, (2014) *"The research of self-balancing vehicle based on posture sensor system"* **Applied Mechanics and Materials *599***: 735–738. DOI: 10.4028/www.scientific.net/AMM.599-601.735.

[21] I. Krzysztofik, J. Takosoglu, and Z. Koruba, (2017) *"Selected methods of control of the scanning and tracking gyroscope system mounted on a combat vehicle"* **Annual Reviews in Control *44***: 173–182. DOI: 10.1016/j.arcontrol.2016.10.003.

[22] J. Xiao, Y. Wang, X. Li, and J. Zheng. "Design of high precision mechatronic-hydraulic leveling system for vehicle-mounted radar". In: *Journal of Physics: Conference Series*. ***2113***. 1. IOP Publishing. 2021, 012041. DOI: 10.1088/1742-6596/2113/1/012041.

[23] C. Lu, D. Huang, Z. Jin, and Y. Huang. "The Research and Design of Auto-leveling Control System for Vehicle-borne Radar Platform Based on AVR". In: *2006 2nd IEEE/ASME International Conference on Mechatronics and Embedded Systems and Applications*. IEEE. 2006, 1–5. DOI: 10.1109/MESA.2006.296949.